

This is an Open Access document downloaded from ORCA, Cardiff University's institutional repository: <https://orca.cardiff.ac.uk/id/eprint/64711/>

This is the author's version of a work that was submitted to / accepted for publication.

Citation for final published version:

Cleall, Peter John , Munoz Criollo, Jose and Rees, Stephen William 2015. Analytical solutions for ground temperature profiles and stored energy using meteorological data. *Transport in Porous Media* 108 (1) , pp. 181-199.

Publishers page: <http://dx.doi.org/10.1007/s11242-014-0395-3>

Please note:

Changes made as a result of publishing processes such as copy-editing, formatting and page numbers may not be reflected in this version. For the definitive version of this publication, please refer to the published source. You are advised to consult the publisher's version if you wish to cite this paper.

This version is being made available in accordance with publisher policies. See <http://orca.cf.ac.uk/policies.html> for usage policies. Copyright and moral rights for publications made available in ORCA are retained by the copyright holders.



Revised September 2014

Title: Analytical solutions for ground temperature profiles and stored energy using meteorological data

Authors: Peter John Cleall¹, José Javier Muñoz-Criollo², Stephen William Rees³

Affiliations:

¹ Corresponding Author and Senior Lecturer, Cardiff School of Engineering, Cardiff University, Cardiff, CF24 3AA, Wales, UK. E-mail: Cleall@cardiff.ac.uk

² Post Graduate Research Student, Cardiff School of Engineering, Cardiff University, Cardiff, CF24 3AA, Wales, UK

³ Lecturer, Cardiff School of Engineering, Cardiff University, Cardiff, CF24 3AA, Wales, UK. E-mail: ReesS@cardiff.ac.uk

Corresponding Author: Dr Peter Cleall
Cardiff School of Engineering
Cardiff University
Cardiff, CF24 3AA
Wales, UK
E-mail: cleall@cardiff.ac.uk
Tel. 029 20875795
Fax. 029 20874004

Abstract

1 Analytical solutions to estimate temperature with depth and stored energy within a soil column
2 based upon readily available meteorological data are presented in this paper which are of
3 particular relevance in the field of ground heat extraction and storage. The transient one-
4 dimensional heat diffusion equation is solved with second kind (Neumann) boundary
5 conditions at the base and third kind (Robin) boundary conditions, based on a heat balance, at
6 the soil surface. In order to describe the soil-atmosphere interactions, mathematical expressions
7 describing the daily and annual variation of solar radiation and air temperature are proposed.
8 The presented analytical solutions are verified against a numerical solution and applied to
9 investigate a case study problem based upon results of a field experiment. It is shown that the
10 proposed analytical approach can offer a reasonable estimate of the thermal behaviour of the
11 soil requiring no information from the soil other than its thermal properties Comparisons of
12 predicted and measured soil temperature profiles and stored energy transients demonstrate
13 there is reasonable overall agreement. The research contributes a practical approach that can
14 provide surface boundary data that is vital in the thermal analysis of many engineering
15 problems. Applications include; inter-seasonal heat transfer, energy piles and other more
16 established ground source heat utilization methods.

17 **Keywords:** Soil, stored energy, thermal, analytical, heat transfer.

18 **1. Introduction**

19 The estimation of ground temperature profiles is important for several engineering applications
20 that use the soil as a reservoir or source of thermal energy. Examples of these applications are
21 the minimisation of thermal losses and passive heating and cooling of buildings (e.g. Rees et
22 al. 2000; Zoras 2009), ground source heating (e.g. Florides and Kalogirou 2007); shallow
23 energy piles (e.g. Wood et al 2010) and inter seasonal thermal energy storage (Bobes-Jesus et
24 al. 2013; Pinel et al. 2011). These applications are highly dependent on the amount of energy
25 present in the near-surface region of the soil and its temporal variation. Subsequently one of
26 the first steps in the process of evaluation of their implementation is related with the assessment
27 of ground temperature profiles and overall ground energy storage. To provide sufficient details
28 such assessments are usually performed with the aid of theoretical models solved by numerical
29 methods (e.g. Qin et al, 2002; Yumrutaş et al. 2005; Laloui et al 2006). These have the
30 advantage of being able to include a high range of complexities within the domain of interest
31 for example, different physical processes, materials, geometries, boundary conditions, etc.
32 However, if the problem is relatively simple, it can be approached analytically. An analytical
33 solution is usually simpler, easier to implement computationally and offers detailed insight
34 about the underlying physical processes. Also, analytical solutions can be helpful in
35 establishing reasonable initial conditions for more comprehensive numerical simulations when
36 no other information is available.

37 Analytical solutions have been applied to solve the diffusion equation and the diffusion-
38 convection equation in soil in various different fields. For example, heat diffusion has been
39 studied in relation to the interaction between buildings and soil (Hagentoft 1996a; Hagentoft
40 1996b; Jacovides et al. 1996, Hollmuller and Lachal, 2014) and the diffusion of contaminants
41 in porous media composed of two or more layers layers (Li and Cleall 2010; Chen et al. 2009).
42 Convection and diffusion have been analysed together in relation with water infiltration (Gao
43 et al. 2003; Wang et al. 2012) and general solute transport in porous media under various
44 boundary conditions (Li and Cleall 2011). Water infiltration in unsaturated soils have also been
45 studied using Richard's equation (Huang and Wu 2012). Approximate analytical solutions
46 have been used to study heat and moisture transfer including phase change (thawing) in soils
47 (Kurylyk, 2014). In each of these approaches three main types of boundary conditions are
48 considered. These are: *first type* (also known as Dirichlet type), which specify the value of the
49 variable at the boundary; *second type* boundary conditions (also known as Neumann type)
50 which specify the value of the derivative of a variable at the boundary; and *third type* boundary

51 conditions (also known as Robin type), these specify both (as a linear combination) the value
52 of the variable and its derivative at the boundary.

53 The limitations of analytical solutions typically result from the simplification of certain aspects
54 of the problem. Some of the first analytical approaches to estimate the temperature of the
55 ground (Michopoulos et al. 2010; Mihalakakou et al. 1997) and coupled heat diffusion and
56 water infiltration (Shao et al. 1998) relied on the assumption of fixed boundary conditions
57 (constant or periodic). These approaches individually achieved objectives of including more
58 than one physical process, more complex geometries (Chuangchid and Krarti 2001) or the
59 actual operation of a heat exchanger used for heating a building (Yumrutaş et al. 2005). In
60 recent years the inclusion of time dependent boundary conditions of the *second type* (Adam
61 and Markiewicz, 2002; Wang 2012; Wang and Bou-Zeid 2012) and of the *third type* (Cleall
62 and Li 2011) has gained more attention to describe in more detail the energy and mass transfer
63 interactions at the soil surface. With regard to the boundary condition at the bottom of the
64 domain it is common to either fix it at an estimated average temperature or assume an insulated
65 (no heat flux) boundary condition. The implication of this last assumption is to neglect any
66 geothermal heat flux. This is typically the case in consideration of the near soil surface (Davies
67 2013), however, where this assumption cannot be made, the inclusion of a constant heat flux
68 at the bottom that takes into account this term is not difficult.

69 This paper presents a new analytical solution to the transient one dimensional heat diffusion
70 equation using a flux boundary condition equal to zero at the bottom of the domain and a *third*
71 *kind* (Robin) boundary condition at its surface. This enables surface heat fluxes directly related
72 to meteorological conditions to be realistically represented. To achieve this, two mathematical
73 expressions for meteorological variables are proposed and compared against daily and hourly
74 experimental meteorological data. These expressions and the proposed analytical solution are
75 then used to consider a field-scale case-study with the results obtained from the analytical
76 solution compared against hourly experimental recordings of soil temperature profiles and
77 estimates of stored energy.

78 **2. Mathematical formulation**

79 **2.1. General Solution**

80 The general form for the one dimensional homogeneous transient heat diffusion equation
81 defined in a finite domain of length L is

82
$$\frac{d^2T}{dz^2} = \frac{1}{\alpha} \frac{dT}{dt} \quad \text{in} \quad \begin{matrix} 0 \leq z \leq L \\ t > 0 \end{matrix} \quad (1)$$

83 where T is the temperature of the soil and α is the thermal diffusivity. The solution of this
 84 equation can be obtained following the approach given in (Özişik 2002) for various boundary
 85 conditions using the integral transform technique. The boundary conditions and initial
 86 condition considered here are defined as:

87
$$f_1(t) = -k \frac{dT}{dz} + h_1 T \quad \text{at} \quad z = 0, t > 0 \quad (2)$$

88
$$f_2(t) = k \frac{dT}{dz} + h_2 T \quad \text{at} \quad z = L, t > 0 \quad (3)$$

89
$$T = F(z) \quad \text{in} \quad 0 \leq z \leq L, t = 0 \quad (4)$$

90 where h_1 and h_2 are the heat transfer coefficient at $z=0$ (soil surface) and $z=L$ respectively, and
 91 k is the soil thermal conductivity. In the case where a Robin boundary condition $f_1(t)$ is applied
 92 at $z=0$, a zero heat flux boundary condition is applied at $z=L$ and a constant initial condition F_i
 93 is used, the solution has the form:

94
$$T(z,t) = \sum_{m=1}^{\infty} 2 \left(\frac{\beta_m^2 + H_1^2}{L(\beta_m^2 + H_1^2) + H_1} \right) e^{-\alpha \beta_m^2 t} \cos \beta_m (L-z) \left[\frac{F_i \sin(\beta_m L)}{\beta_m} + \frac{\alpha \cos(\beta_m L)}{k_1} \int_{t'=0}^t e^{\alpha \beta_m^2 t'} f_1(t') dt' \right] \quad (5)$$

95 where $H_1 = h_1/k$ and the eigenvalues β_m are the positive roots of:

96
$$\beta \tan \beta = H_1 \quad (6)$$

97 **2.2 Energy stored in the soil**

98 The description of the soil's temperature profile with depth given by equation (5) allows the
 99 calculation of the energy stored (J/m^2) in a column of soil of depth L with reference to the
 100 energy present in the soil at an arbitrary reference time as:

101
$$Q(z,t) = \rho c_p \int_0^L [T(z,t) - T(z,t_{ref})] dz \quad (7)$$

102 where ρ and c_p are the density and specific heat capacity of the soil, $T(z,t)$ is the temperature
 103 profile at time t and $T(z,t_{ref})$ is the temperature profile at a reference time t_{ref} .

104

105 **2.3. Boundary condition at the soil surface**

106 The boundary condition at the soil surface ($z=0$) is based on consideration of the heat energy
 107 balance at the surface of the soil and can be defined by:

$$108 \quad -k \frac{dT}{dz} = (1 - \alpha_s)R + 4\sigma T_{0,K}^3 \varepsilon_G \varepsilon_{sky}^{0.25} T_{a,K} - 4\sigma T_{0,K}^3 \varepsilon_G T_K + h_E(q_a - q_G) + h_C T_a - h_C T \quad (8)$$

109 where α_s is the soil albedo (Garratt 1994), R (W/m^2) is solar radiation, σ ($\text{W/m}^2\text{K}^4$) is the
 110 Steffan-Boltzmann constant, T_a and $T_{a,K}$ is air temperature in ($^\circ\text{C}$) and (K) respectively,
 111 (variables and constants used to calculate the terms in equation (8) are summarized in Table
 112 1). $T_{0,K}$ (K) is an average temperature that arises from the linearization of the infrared heat
 113 transfer equation (Duffie and Beckman 2006) and is defined as:

$$114 \quad T_{0,K} = \left[0.25 (\varepsilon_{sky}^{0.5} T_{a,K}^2 + T_{G,K}^2) (\varepsilon_{sky}^{0.25} T_{a,K} + T_{G,K}) \right]^{1/3} \quad (9)$$

115 $T_{G,K}$ is the temperature of the soil surface in (K), ε_G is the emissivity of the soil surface (Garratt
 116 1994), ε_{sky} is the sky emissivity (Edinger and Brady 1974; Herb et al. 2008) defined as:

$$117 \quad \varepsilon_{sky} = n + 0.67(1-n)(q_a / 100)^{0.08} \quad (10)$$

118 where n is a cloud factor with a non-dimensional value from 0 to 1. q_G (Pa) and q_a (Pa) are the
 119 vapour pressure for the soil surface and air respectively and are defined as:

$$120 \quad q_G = \exp\left(\frac{\psi M_{H_2O} g}{RT_{G,K}}\right) 611 \exp\left(\frac{L_v M_{H_2O}}{R} \left(\frac{1}{273.15K} - \frac{1}{T_{G,K}}\right)\right) \quad (11)$$

$$121 \quad q_a = \left(\frac{H_r}{100}\right) 611 \exp\left(\frac{L_v M_w}{R} \left(\frac{1}{273.15K} - \frac{1}{T_{a,K}}\right)\right) \quad (12)$$

122 where ψ is the surface water pressure in (m) (the average value of saturation and wilting point
 123 for clay provided in (Garratt 1994) is used), M_w is the molecular weight of water (kg/mol), g
 124 (m/s^2) is the acceleration of gravity, R (J/molK) is the gas constant, L_v (J/kg) is the latent heat
 125 of vaporization of water and H_r (%) is the relative humidity. An expression for the saturation
 126 vapour pressure can be found in (North and Erukhimova 2009), while the term for the relative
 127 humidity of the soil is defined in (Philip and de Vries 1957).

128 The heat transfer coefficients for evaporative (h_E) and convective (h_C) heat flux can be defined
 129 following the approach given by (Jansson et al. 2006). This approach assumes a turbulent heat

130 transfer process in the surface of the soil and has the advantage of using relatively simple heat
 131 transfer coefficients:

$$132 \quad h_E = \frac{\rho_a L_v}{r_a} \quad (13)$$

$$133 \quad h_C = \frac{\rho_a c_p}{r_a \eta} \quad (14)$$

134 where ρ_a (kg/m³) is the air density, c_p (J/kgK) is air specific heat capacity, η (Pa/K) is the
 135 psychrometric constant and r_a (s/m) is the aerodynamic resistance defined (for neutral
 136 conditions (Garratt 1994)) as:

$$137 \quad r_a = \frac{\log\left(\frac{z_{ref}}{z_{mr}}\right) \log\left(\frac{z_{ref}}{z_{hr}}\right)}{k_{vk}^2 u} \quad (15)$$

138 where u (m/s) is the wind velocity, k_{vk} is the Von Karman constant, z_{ref} (m) is the height at
 139 which wind speed and air temperature measurements were made, z_{mr} and z_{hr} (m) are the relative
 140 roughness for momentum and heat respectively of the soil surface in its interaction with the
 141 atmospheric boundary and their values are taken from (Garratt 1994) and (Kotani and Sugita
 142 2005) respectively. The psychrometric constant is defined as:

$$143 \quad \eta = \frac{c_{p,a} P M_a}{L M_w} \quad (16)$$

144 where P is the atmospheric pressure (Pa) and M_a is the molecular weight of air (kg/mol). Others
 145 (Edinger and Brady 1974; Herb et al. 2008) use different approaches to define these heat
 146 transfer coefficients which are useful for cases where non turbulent processes can be assumed
 147 (low wind speeds) that take into account forced and natural convection, however these
 148 coefficients are, relatively more complex and not readily amenable for inclusion in the form of
 149 analytical solution presented here.

150 Equation (8) can be rewritten in the form of equation (2), to subsequently be used in the solution
 151 of equation (5). For this, average values for air temperature, wind speed and relative humidity
 152 are required to calculate some of these coefficients (namely ε_{sky} , $T_{0,K}$ and q_a) that otherwise
 153 would be unsuitable to include in an analytical approach. Also, the evaporative term q_G is
 154 dependent on the temperature of the surface of the soil. An average temperature for the soil
 155 surface can be estimated by integrating equation (8) over a full yearly cycle so as to consider a

156 quasi-equilibrium scenario (i.e. zero net heat flux) after expressions for solar radiation and air
157 temperature have been defined.

158 **2.4. Mathematical expressions for meteorological variables**

159 In order to solve equation (5) using equation (8) as a boundary condition it is necessary to
160 formulate expressions for the meteorological variables required. Mathematical expressions for
161 solar radiation are available in the literature (Duffie and Beckman 2006). In general these
162 expressions are functions of geographical parameters and provide the amount of radiation
163 between sunrise and sunset, however, they are not suitable for use here because for a continuous
164 analytical solution a function that is applicable during night time is required. In this paper we
165 offer two simplified mathematical expressions for idealised daily and annual variations of solar
166 radiation and air temperature that can be constructed using widely available averaged
167 meteorological data.

168 The expression for solar radiation builds upon another expression for daily variations given in
169 the literature (Lumb 1964). Here this expression is expanded to include annual variation. An
170 equation for variation in solar radiation is proposed here as:

$$171 \quad R(t) = \frac{\pi}{2} \left(\cos^2(\gamma t) - \cos(\gamma t) + \frac{4 - \pi}{2\pi} \right) (R_1 \cos(\varphi t) + R_2) \quad (17)$$

172 where t is given in seconds taking the origin at midyear (July 1st), φ is the annual period defined
173 as $2\pi/31557600$ s (2π divided by 365.25 days in seconds), and γ is the daily period defined as
174 $2\pi/86400$ s (2π divided by 24 hours in seconds). R_1 and R_2 are coefficients, that can be
175 determined from the meteorological conditions for summer and winter (the summer and winter
176 periods can be arbitrarily defined based on localised conditions). These coefficients are defined
177 as:

$$178 \quad R_1 = 0.5(A - B) \quad (18)$$

$$179 \quad R_2 = 0.5(A + B) \quad (19)$$

180 where A and B are the summer and winter daily average solar radiation respectively.

181 A similar sinusoidal expression is proposed to represent the diurnal air temperature variation
182 as in general air temperature variations correlate to insolation. For simplicity a sinusoidal daily
183 variation with its maximum at midday and the minimum at midnight is assumed. The annual
184 variation is mainly sinusoidal with maximums and minimums at summer and winter

185 respectively but incorporates an additional sine term to take into account typically observed
 186 slightly higher values in spring and slightly lower values in autumn. The proposed expression
 187 is:

$$188 \quad T_a(t) = T_1[\cos(\varphi t) + 0.5\sin(\varphi t)] + T_2 - \{T_3[\cos(\varphi t) + 0.5\sin(\varphi t)] + T_4\} \cos(\gamma t) \quad (20)$$

189 where t is given in seconds taking the origin at midyear (1st July). T_1 , T_2 , T_3 and T_4 are
 190 coefficients determined from the meteorological conditions for mid-summer and mid-winter
 191 periods. They are calculated as:

$$192 \quad T_1 = 0.5(C - D) \quad (21)$$

$$193 \quad T_2 = 0.5(C + D) \quad (22)$$

$$194 \quad T_3 = (E - F) \quad (23)$$

$$195 \quad T_4 = 0.5(E + F) \quad (24)$$

196 where coefficients C , D , E , F are defined as the mid-summer daily average, mid-winter daily
 197 average, mid-summer average amplitude, and mid-winter average amplitude respectively.

198 The average value for solar radiation and air temperature defined by these mathematical
 199 expressions can be calculated by averaging equations (17) and (20) over a suitable period of
 200 time (e.g. four years). It can be found that the average value for solar radiation and air
 201 temperature is given by R_2 and T_2 respectively.

202 Due to the relatively random nature of variations in relative humidity and wind speed across
 203 an annual time span, mathematical expressions for these variables have not been developed
 204 and instead it is proposed that annual averages based on values from meteorological data sets
 205 are used.

206 **3. Verification**

207 The analytical solution proposed here is verified via consideration of a hypothetical problem.
 208 The results obtained from the analytical solutions are compared with those from a numerical
 209 solution using the finite-element method (Cleall et al. 2007; Seetharam et al. 2007). A number
 210 of analyses have been undertaken with varying values of material parameter and system
 211 coefficients to investigate the uniqueness of the solutions. Results of a typical analysis follow.

212 Problem statement: A 20 m deep layer of soil is defined with an initially uniform temperature
 213 of 14 °C. Hypothetical soil material parameters ($k= 1 \text{ W/mK}$, $c_p= 800 \text{ J/kgK}$, $\rho= 2000 \text{ kg/m}^3$),
 214 values for the coefficients of equations (17) and (20) ($A= 250 \text{ W/m}^2$; $B= 20 \text{ W/m}^2$; $C= 16 \text{ °C}$;
 215 $D= 3.6 \text{ °C}$; $E= 2.5 \text{ °C}$; $F= 5 \text{ °C}$), an average value for soil surface temperature of 8.7 °C
 216 (calculated, as explained before, by integrating equation (8) over a full yearly cycle), a cloud
 217 factor of 0 and annual averages of relative humidity (80.6 %) and wind speed (1.14 m/s) are
 218 assumed. The finite element analysis discretised the domain with 512 2-noded equally sized
 219 elements and used a constant time step of 1800 seconds, full details of the numerical approach
 220 used can be found in Seetharam et al (2007). Comparison of the temperature profiles and
 221 energy stored obtained from both the proposed solution and the alternative numerical solution
 222 are presented in figures 1 and 2 for the 1st, 40th, and 80th year of analysis.

223 Figure 1 compares analytical and numerical temperature profiles for 4 sampling dates for 3
 224 different years. The year is taken to comprise 365.25 days and the sampling points have been
 225 homogeneously distributed in each year and approximately correspond to calendar dates of 1st
 226 January (t1), 1st April (t2), 1st July (t3) and 1st October (t4). It can be seen that the analytical
 227 and numerical results are in excellent agreement and that the temperature profiles for the 40th
 228 and 80th years are identical implying that a stationary state has been reached.

229 Figure 2 shows the comparison of stored energy, for year 40th, calculated analytically using
 230 equation (7) and numerically using:

$$231 \quad Q_N(z_i, t_j) = \rho C_p \sum_{i=0}^m [T_N(z_i, t_j) - T(z_i, t_{ref})] \Delta z_i \quad (25)$$

232 where Δz_i is the length of cell i . In both cases, analytical and numerical, a constant reference
 233 temperature of 8.7 °C (the temperature at the bottom of the domain at year 40th) has been used.
 234 The maximum relative error between numerical and analytical is less than 0.1%. Again it can
 235 be seen that the analytical and numerical results are in excellent agreement.

236 **4. Application to a case-study**

237 A two year long demonstration project commissioned by the British Highways Agency in order
 238 to assess the feasibility of use of inter-seasonal heat storage systems to provide thermal
 239 maintenance to highways and heating for buildings was reported by the Transport Research
 240 Laboratory (TRL) (Carder et al. 2007). The project was carried out between July 2005 and
 241 May 2007 at Toddington, UK. Boreholes up to 12.875 m deep were drilled and temperature

242 sensor arrays placed inside. Two of these boreholes were located far from the location of the
243 storage system, and served as control boreholes, the remaining boreholes were distributed on a
244 highway section and recorded the ground temperature evolution through time while the inter-
245 seasonal heat storage system was active. The specific data used for this work corresponds to
246 one of the control boreholes, and as such the storage system need not be considered further.
247 No details regarding regular surface maintenance above this borehole (e.g. grass cutting) are
248 provided in (Carder et al. 2007). However site visits by the authors indicate it is reasonable to
249 assume that the surface was subject to a natural cycle of plant growth (mainly grass).

250 TRL set up a meteorological station and performed recordings of solar radiation, air
251 temperature, wind speed, relative humidity and precipitation every 15 minutes from July 2005
252 to May 2007 (Carder et al. 2007). Hourly average values from this station are used in this work
253 to compare against results obtained from the mathematical expressions proposed to describe
254 the meteorological conditions. This approach offers the advantage of testing the ability of the
255 proposed expressions, fitted to readily available long term meteorological data, to represent
256 localised short term measured data.

257 The proposed mathematical expressions for solar radiation and air temperature have been fitted
258 to meteorological data recordings reported by the British Atmospheric Data Centre (UK
259 Meteorological Office 2012) and the Met Office (UK Meteorological Office) for the period
260 from 1985 to 2004 to investigate their appropriateness and ability to represent realistically the
261 diurnal and seasonal variations. For the purpose of this work, a monitoring station located in
262 Hertfordshire, UK (coordinates 51.8062 latitude, -0.3585 longitude) was selected as it offers
263 suitable daily and hourly meteorological data and is also relatively near (17 km) to the site of
264 the experimental project for which localised meteorological data and soil temperature profiles
265 were also recorded. The variables obtained to allow calculation of the coefficients used in the
266 mathematical expressions for solar radiation (17) and air temperature (20) are summarized in
267 Tables 2 and 3. These variables represent average values for mid-summer and mid-winter
268 periods which in this study are defined respectively as from 25th June to 5th July and from
269 25th December to 5th January. These periods were chosen since they are expected to contain
270 the maximum and minimum values of the variables. Due to data availability, cloud cover
271 information was obtained from a monitoring station located at Bedford (coordinates 52.2265
272 latitude, -0.46376 longitude, approx. 31 km from the experimental site). The station has
273 reported hourly cloud cover data from November 2008 allowing the determination of an

274 average cloud factor value of 0.59 for the five year period (2009-2013). It is assumed that this
275 value is representative of the amount of cloud cover present in any other year.

276 Annual averages of relative humidity (80.6 %) and wind speed (1.14 m/s) based on values
277 recorded during the two-year long (2005-2006) demonstration project are used in the
278 subsequent application of the proposed analytical solution to consider a 20 m deep soil column.
279 The proposed solution also requires a set of material parameters to describe the soil thermal
280 properties these have been based on those reported in (Carder et al. 2007) for the soil at this
281 site and are summarised in Table 4.

282 **5. Results**

283 Figure 3 and 4 present comparisons of daily average values generated with the proposed
284 mathematical expressions for solar radiation (equation (17)) and air temperature (equation (20))
285 with equivalent measured data for the period 1985-2004. In both cases it can be observed that the
286 predicted data are constrained by the well-defined maximums and minimums. These values, as
287 discussed before, are based on the average values for summer and winter. As would be expected
288 the data with higher daily average values for solar radiation correspond to summer months
289 while those with lower values correspond to winter months. It can also be seen that in each
290 month the experimental data tend to have a wider range of lower values this is because the
291 mathematical expression for the predicted data is idealized and in no way takes into account
292 the effect of cloud cover which will decrease the amount of solar radiation that reaches the soil
293 surface. These effects result in the spread of data points displayed in figure 3 having a
294 trapezoidal like shape. As before, the data with the higher average values of daily temperature
295 shown in figure 4 correspond to summer months while those with lower values correspond to
296 winter months. It can be seen that the predicted data for air temperature offer a better
297 comparison with the ideal line included in the figure and that it offers a better correlation factor
298 than the case for solar radiation. This is probably due to the fact that air temperature is not as
299 highly impacted by the presence of cloud cover. It is noted that if the average value for
300 maximum daily summer temperatures and the average value for minimum daily winter
301 temperatures are used an improved linear fit in figure 4 could be obtained. However daily
302 averages for summer and winter have been used to retain homogeneity with the definition of
303 coefficients for solar radiation. Implementation of averaged values in the proposed solution is
304 trivial (i.e. simply by revising the definition of the coefficients of equation (20)) and either
305 approach can be adopted to achieve the best fit with measured data.

306 Figures 5 and 6 present comparisons of experimental and predicted daily average values for
307 solar radiation and air temperature respectively for 2005-2006. This permits testing of the
308 proposed expressions for solar radiation and air temperature with an independent subset of
309 data. The experimental values shown are taken from (UK Meteorological Office 2012; UK
310 Meteorological Office). It can be seen that the correlation values are in general similar to those
311 obtained for the period 1985-2004 which was used to establish the coefficients in the
312 expressions.

313 Fig. 7 and Fig. 8 present comparisons of hourly values of solar radiation and air temperature
314 from the proposed expressions with equivalent data recorded on site by TRL (Carder et al.
315 2007) from September 2005 to August 2006. In Fig. 7 a pattern of stratification of the data
316 points can be observed with data points forming horizontal bands. These 'bands' are mostly
317 composed for points belonging to summer months. They arise because as equation (17)
318 approaches its maximum in mid-summer it tends to flatten and predict similar values for
319 corresponding hours from mid-May to mid-August while the experimental values are affected
320 by the relatively random presence of clouds.

321 Fig. 8 shows experimental and predicted hourly air temperature values. A general trend of
322 underestimation of the predicted temperatures can be observed. It is worth noting that the
323 period considered was warmer (on average by 0.5 °C) than for the previous 20 years. In
324 particular, the average air temperature for the last 20 years was 9.7 °C while the average air
325 temperature for 2005-2006 calculated using TRL data was 10.2 °C. These differences are more
326 marked if they are considered at a monthly level, where the average for July and January for
327 the last 30 years was 16.2 °C and 4.1 °C respectively and 20 °C and 3.4 °C for July 2006 and
328 January 2006 respectively. This in part explains the general under prediction of temperatures
329 seen in Fig. 8. It can also be observed in figure 7 that a limited number of small negative night
330 time values are given by equation (17) due to its sinusoidal and continuous nature, this is
331 illustrated more clearly in Fig. 9. These unavoidable limitations are acknowledged but it is
332 noted that the overall daily solar radiation is still realistic as seen in Fig. 3 where the negative
333 values are absent as it is presenting averaged daily values. Fig. 9 also illustrates the effect of
334 clouds as well as the effect of variation of day length.

335 Fig. 10 and Fig. 11 show the comparison of soil temperatures obtained by applying equations
336 (17) and (20) in equation (5) (using the material data provided in Table 4 and a domain depth
337 of 20 m) against experimental data from a control borehole of TRL for three different depths.

338 An average cloud factor of 0.59 has been used in equation (10) to take into account the effect
339 of clouds in the infrared terms in equation (8) Fig. 10 shows the comparison for the temperature
340 sensor at 0.025 m. Although the correlation factor tends to be low due to the random nature of
341 the experimental data caused in part by the random nature of the daily meteorological data, it
342 can be seen that the analytical solution offers a reasonable description of the thermal behaviour
343 of the soil.

344 Fig. 11 shows the comparison for the temperature sensors located at 1.025 m and 12.875 m.
345 These results indicate that as the depth increases the correlation factor tend to increase.
346 However, for deeper sections of the soil this trend no longer holds, this is due to the fact that
347 the temperature variations in the ground are very small. At depth of 12.875 m, where it would
348 be expected that the soil would maintain at a relatively constant value the analytical solution
349 proposed in this work reasonably predicts the experimental value with a maximum error of 1.3
350 °C. It is worth noting that the proposed model assumes a homogeneous free heat flux boundary
351 condition at the bottom of the soil column which is at a depth of 20 m. The advantage of this
352 approach over one that considers a first type (Dirichlet) boundary condition at the base is that
353 no assumption of soil temperature at depth is required.

354 Transient variations in stored energy can be obtained via use of equation (7) and consideration
355 of measured temperature profiles. As the experimental temperatures are discrete data, linear
356 interpolation is used to approximate continuous profiles. Fig. 12 shows comparisons of the
357 calculated and estimated measured stored energy in a column of soil 12.875 m deep. It can be
358 observed that the proposed model is able to offer realistic estimates in the relative change in
359 seasonal energy storage. It is noted that there is a trend of a slight underestimation of energy
360 stored. This is related to the fact that the period compared, as mentioned previously, was
361 slightly warmer than the longer term average of the period used to calibrate equations that
362 represent the surface weather condition.

363 **6. Conclusions**

364 Analytical solutions to estimate the soil temperature with depth and stored energy were
365 presented in this paper. The boundary conditions used are of the *second kind* (Neumann) at the
366 bottom and of the *third kind* (Robin) based on a heat balance at the soil surface. In order to
367 describe the soil-atmosphere interactions, mathematical expressions describing the daily and
368 annual variation of solar radiation and air temperature have been proposed. The analytical
369 solutions were shown to correlate well with numerical solutions from a finite-element analysis.

370 The presented analytical solutions were used to investigate a case study problem base upon
371 results of a field experiment reported by others. Predicted soil temperature profiles and stored
372 energy transients have been compared against experimental recordings for over one year. Also
373 the predicted meteorological data has been compared against widely available public records
374 and against data recorded on site. The main differences found between the predicted and
375 experimental data are due to the random nature of certain meteorological variables (e.g. clouds)
376 and the inevitable variability in average data for a particular year in comparison to averages
377 from a longer term data set. The results show that the analytical approach proposed can offer a
378 reasonable estimate of the thermal behaviour of the soil requiring no information from the soil
379 other than its thermal properties. This work provides a useful tool in applications requiring
380 estimations of the soil temperature profiles, for example in the field of ground heat extraction
381 and storage, or in numerical problems where a reasonable initial state can minimise the
382 computational time to reach a convergent steady state.

383 **Acknowledgments**

384 The authors gratefully acknowledge the support given to the second author whose PhD studies
385 were funded by CONACYT (the Mexican National Council of Science and Technology) and
386 SEP (Mexican Secretariat of Public Education). Also the supply by TRL/HA of the source
387 data published in (Carder et al. 2007) is gratefully acknowledged.

388 **References**

- 389 Adam D, Markiewicz R. Nutzung der geothermischen energie mittels erdberuhrter
390 bauwerke. Osterr Ing Archit;147, (2002)
- 391 Bobes-Jesus, V., Pascual-Muñoz, P., Castro-Fresno, D., Rodriguez-Hernandez, J.: Asphalt
392 solar collectors: A literature review. Appl. Energy. 102, 962–970 (2013).
- 393 Carder, D.R., Barker, K.J., Hewitt, M.G., Ritter, D., Kiff, A.: Performance of an interseasonal
394 heat transfer facility for collection, storage and re-use of solar heat from the road surface.
395 (2007).
- 396 Chen, Y., Xie, H., Ke, H., Chen, R. An analytical solution for one-dimensional contaminant
397 diffusion through multi-layered system and its applications Environmental Geology, 58(5),
398 1083-1094, (2009)

- 400 Chuangchid, P., Krarti, M.: Foundation heat loss from heated concrete slab-on-grade floors.
401 *Build. Environ.* 36, 637–655 (2001).
- 402 Cleall, P.J., Li, Y.-C.: Analytical Solution for Diffusion of VOCs through Composite Landfill
403 Liners. *J. Geotech. Geoenvironmental Eng.* 137, 850–854 (2011).
- 404 Cleall, P.J., Seetharam, S.C., Thomas, H.R.: Inclusion of some aspects of chemical behavior
405 of unsaturated soil in thermo/hydro/chemical/mechanical models. I: Model development. *J.*
406 *Eng. Mech.-Asce.* 133, 338–347 (2007).
- 407 Davies, J.H.: Global map of solid Earth surface heat flow. *Geochem. Geophys. Geosystems.*
408 14, 4608–4622 (2013).
- 409 Duffie, J.A., Beckman, W.A.: *Solar Engineering of Thermal Processes.* Wiley (2006).
- 410 Edinger, J.E., Brady, D.K.: *Heat Exchange and Transport in the Environment.* John Hopkins
411 University (1974).
- 412 Florides, G., Kalogirou, S.: Ground heat exchangers—A review of systems, models and
413 applications. *Renew. Energy.* 32, 2461–2478 (2007).
- 414 Gao, Z., Fan, X., Bian, L.: An analytical solution to one-dimensional thermal conduction-
415 convection in soil. *Soil Sci.* 168, 99–107 (2003).
- 416 Garratt, J.R.: *The Atmospheric Boundary Layer.* Cambridge University Press (1994).
- 417 Hagentoft, C.E.: Heat losses and temperature in the ground under a building with and without
418 ground water flow .1. Infinite ground water flow rate. *Build. Environ.* 31, 3–11 (1996)(a).
- 419 Hagentoft, C.E.: Heat losses and temperature in the ground under a building with and without
420 ground water flow .2. Finite ground water flow rate. *Build. Environ.* 31, 13–19 (1996)(b).
- 421 Herb, W.R., Janke, B., Mohseni, O., Stefan, H.G.: Ground surface temperature simulation for
422 different land covers. *J. Hydrol.* 356, 327–343 (2008).
- 423 Hollmuller P. and Lachal B.: Air–soil heat exchangers for heating and cooling of buildings:
424 Design guidelines, potentials and constraints, system integration and global energy balance.
425 *Applied Energy.* 119, 476–487, (2014).

426 Huang, R.Q., Wu, L.Z.: Analytical solutions to 1-D horizontal and vertical water infiltration in
427 saturated/unsaturated soils considering time-varying rainfall. *Comput. Geotech.* 39, 66–72
428 (2012).

429 Jacovides, C.P., Mihalakakou, G., Santamouris, M., Lewis, J.O.: On the ground temperature
430 profile for passive cooling applications in buildings. *Sol. Energy.* 57, 167–175 (1996).

431 Jansson, C., Almkvist, E., Jansson, P.: Heat balance of an asphalt surface: observations and
432 physically-based simulations. *Meteorol. Appl.* 13, 203–212 (2006).

433 Kotani, A., Sugita, M.: Seasonal variation of surface fluxes and scalar roughness of suburban
434 land covers. *Agric. For. Meteorol.* 135, 1–21 (2005).

435 Kurylyk, B. L., McKenzie, J. M., MacQuarrie, K. T. B., Voss, C. I.: Analytical solutions for
436 benchmarking cold regions subsurface water flow and energy transport models: One-
437 dimensional soil thaw with conduction and advection. *Advances in Water Resources.* 70, 172–
438 184 (2014).

439 Laloui, L., Nuth, M., Vulliet, L. Experimental and numerical investigations of the behaviour
440 of a heat exchanger pile. *International Journal for Numerical and Analytical Methods in*
441 *Geomechanics*, 30 (8), 763-781 (2006)

442 Li, Y.-C., Cleall, P.J.: Analytical Solutions for Contaminant Diffusion in Double-Layered
443 Porous Media. *J. Geotech. Geoenvironmental Eng.* 136, 1542–1554 (2010).

444 Li, Y.-C., Cleall, P.J.: Analytical solutions for advective–dispersive solute transport in double-
445 layered finite porous media. *Int. J. Numer. Anal. Methods Geomech.* 35, 438–460 (2011).

446 Lumb, F.E.: The influence of cloud on hourly amounts of total solar radiation at the sea
447 surface. *Q. J. R. Meteorol. Soc.* 90, 43–56 (1964).

448 Michopoulos, A., Papakostas, K.T., Mavrommatis, T., Kyriakis, N.: Comparative assessment
449 of eight models predicting the ground temperature. *JP J. Heat Mass Transf.* 4, 119–135 (2010).

450 Mihalakakou, G., Santamouris, M., Lewis, J.O., Asimakopoulos, D.N.: On the application of
451 the energy balance equation to predict ground temperature profiles. *Sol. Energy.* 60, 181–190
452 (1997).

453 North, G.R., Erukhimova, T.L.: Atmospheric Thermodynamics: Elementary Physics and
454 Chemistry. Cambridge University Press (2009).

455 Özişik, N.: Boundary Value Problems of Heat Conduction. Dover Publications, Incorporated
456 (2002).

457 Philip, J.R., de Vries, D.A.: Moisture movement in porous materials under temperature
458 gradients. *Trans. Am. Geophys. Union.* 38, 222–232 (1957).

459 Pinel, P., Cruickshank, C.A., Beausoleil-Morrison, I., Wills, A.: A review of available methods
460 for seasonal storage of solar thermal energy in residential applications. *Renew. Sustain. Energy*
461 *Rev.* 15, 3341–3359 (2011).

462 Qin, Z., Berliner, P., Karnieli, A.: Numerical solution of a complete surface energy balance
463 model for simulation of heat fluxes and surface temperature under bare soil environment.
464 *Applied Mathematics and Computation.* 130 (1), 171–200 (2002).

465 Rees, S.W., Adjali, M.H., Zhou, Z., Davies, M., Thomas, H.R.: Ground heat transfer effects on
466 the thermal performance of earth-contact structures. *Renew. Sustain. Energy Rev.* 4, 213–265
467 (2000).

468 Seetharam, S.C., Thomas, H.R., Cleall, P.J.: Coupled thermo/hydro/chemical/mechanical
469 model for unsaturated soils—Numerical algorithm. *Int. J. Numer. Methods Eng.* 70, 1480–
470 1511 (2007).

471 Shao, M., Horton, R., Jaynes, D.B.: Analytical solution for one-dimensional heat conduction-
472 convection equation. *Soil Sci. Soc. Am. J.* 62, 123–128 (1998).

473 UK Meteorological Office: Met Office Integrated Data Archive System (MIDAS) Land and
474 Marine Surface Stations Data (1853-current),
475 http://badc.nerc.ac.uk/view/badc.nerc.ac.uk__ATOM__dataent_ukmo-midas.

476 UK Meteorological Office: Met Office: UK climate summaries,
477 <http://www.metoffice.gov.uk/climate/uk/index.html>.

478 Wang, L., Gao, Z., Horton, R., Lenschow, D.H., Meng, K., Jaynes, D.B.: An Analytical
479 Solution to the One-Dimensional Heat Conduction–Convection Equation in Soil. *Soil Sci. Soc.*
480 *Am. J.* 76, 1978–1986 (2012).

- 481 Wang, Z.-H.: Reconstruction of soil thermal field from a single depth measurement. *J. Hydrol.*
482 464–465, 541–549 (2012).
- 483 Wang, Z.-H., Bou-Zeid, E.: A novel approach for the estimation of soil ground heat flux.
484 *Agric. For. Meteorol.* 154–155, 214–221 (2012).
- 485 Wood, C.J., Liu, H., Riffat, S.B. An investigation of the heat pump performance and ground
486 temperature of a piled foundation heat exchanger system for a residential building, *Energy*,
487 35(12), 4932–4940 (2010)
- 488 Yumrutaş, R., Kanoğlu, M., Bolatturk, A., Bedir, M.Ş.: Computational model for a ground
489 coupled space cooling system with an underground energy storage tank. *Energy Build.* 37,
490 353–360 (2005).
- 491 Zoras, S.: A Review of Building Earth-Contact Heat Transfer. *Adv. Build. Energy Res.* 3,
492 289–314 (2009).

493 **Table 1 - Summary of variables and constants used to calculate parameters in equation**
 494 **(11)**

ρ_a (kg/m ³)	1.2041	L_v (J/kg)	2.45E6	z_{mr} (m)	1E-3
$c_{p,a}$ (J/kgK)	1012	z_{ref} (m)	3	z_{hr} (m)	1E-3
k_{vk}	0.41	P (Pa)	101325	M_w (kg/mol)	0.0180153
M_a (kg/mol)	0.02897	ψ (m)	-75.2025	R (J/molK)	8.3144621
g (m/s ²)	9.8	α_s	.15	σ (W/m ² K ⁴)	5.67E-8
ε_G	0.97				

495

496 **Table 2: Summary of values used to calculate coefficients for the mathematical**
 497 **expression for solar radiation equation (17). Based on data from (UK Meteorological**
 498 **Office 2012)**

A	Mid-summer daily average	204.2 W/m ²
B	Mid-winter daily average	21.3 W/m ²

499

500 **Table 3: Summary of values used to calculate coefficients for the mathematical**
 501 **expression for air temperature equation (20). Based on data from (UK Meteorological**
 502 **Office 2012).**

C	Mid-summer daily average	15.4 °C
D	Mid-winter daily average	3.6 °C
E	Mid-summer average amplitude	2.7 °C
F	Mid-winter average amplitude	4.2 °C

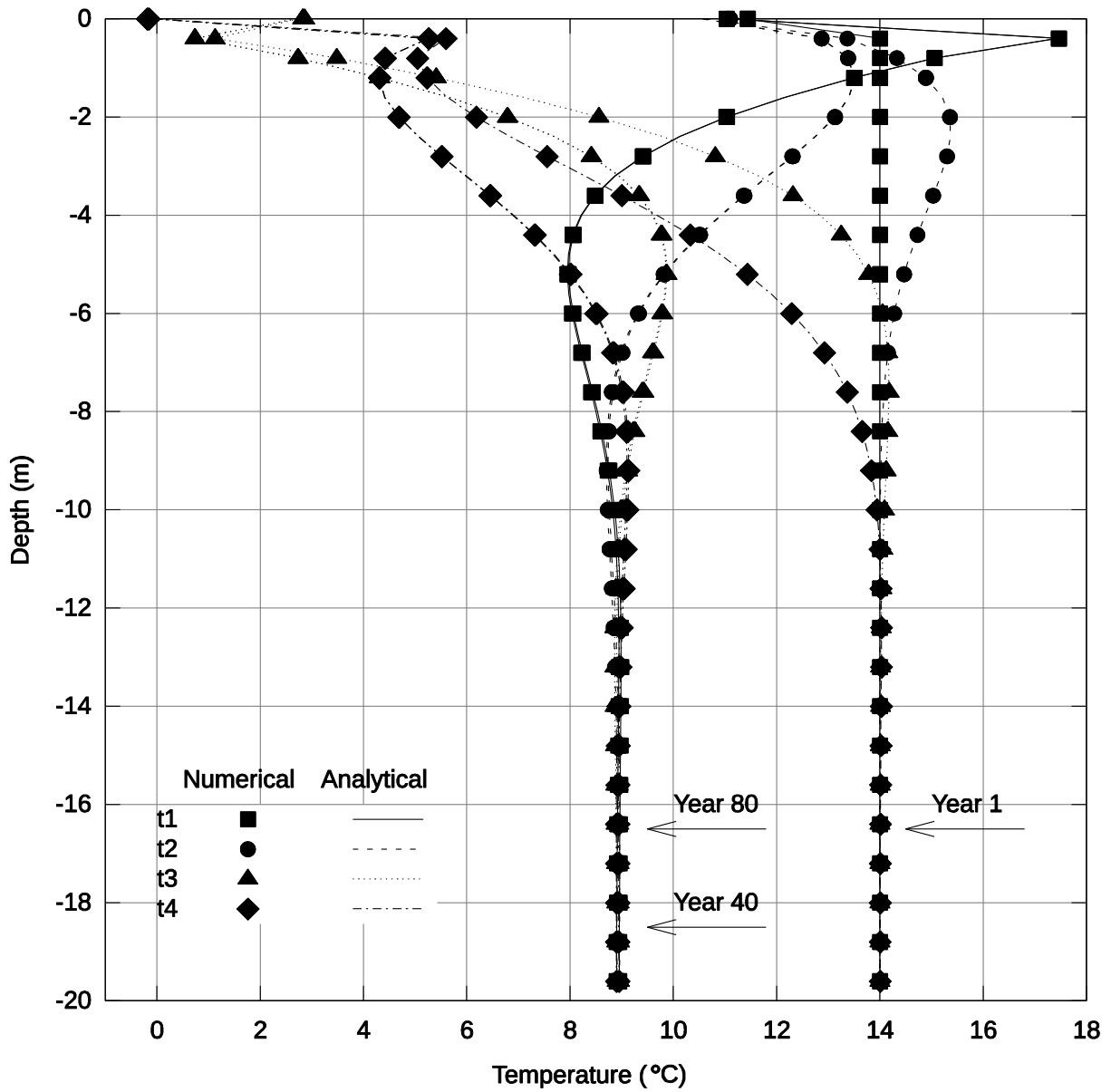
503

504 **Table 4: Soil material parameters (Carder et al. 2007) and domain depth.**

k	Soil thermal conductivity	1.2 W/mk
ρ	Soil density	1960 kg/m ³
c_p	Soil specific capacity	840 J/kgK
α	Soil thermal diffusivity ($=k/\rho c_p$)	
L	Depth of the domain	20 m

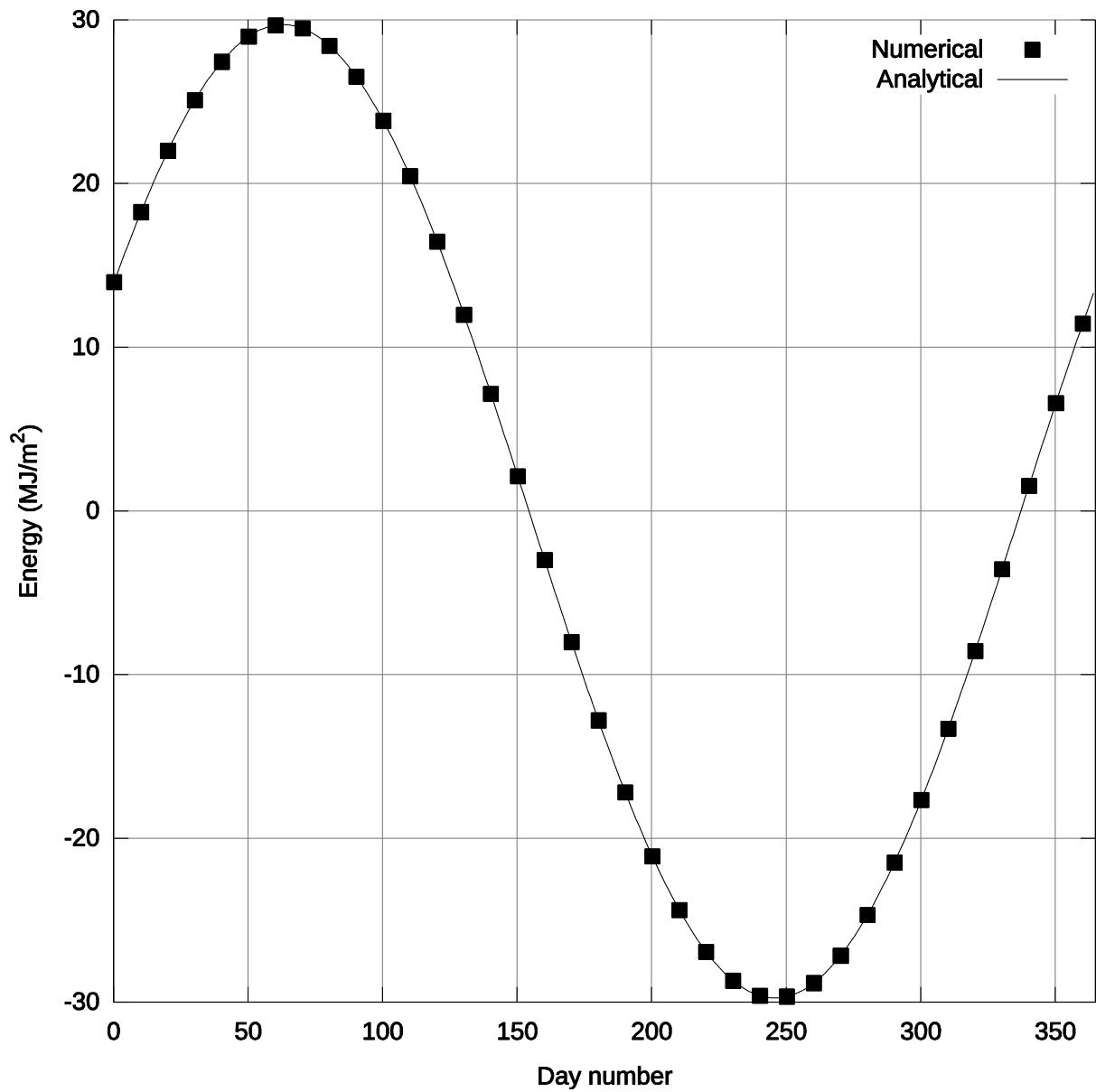
505

Figure Captions



507

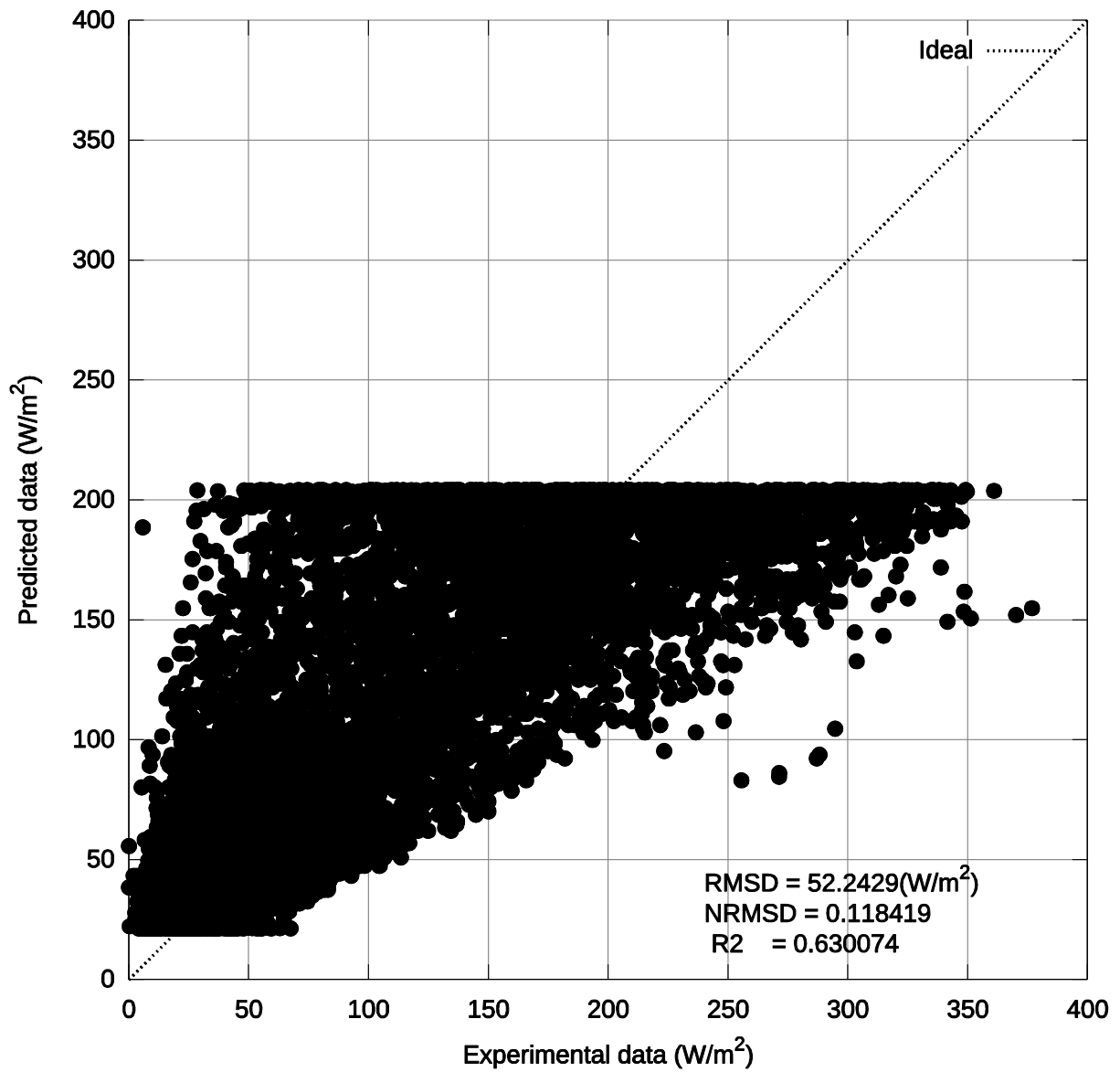
508 **Fig. 1** Comparison of analytical and numerical results for 4 dates for 3 different years (1st, 40th
 509 and 80th). 1st January (t1), 1st April (t2), 1st July (t3) and 1st October (t4) of each year



510

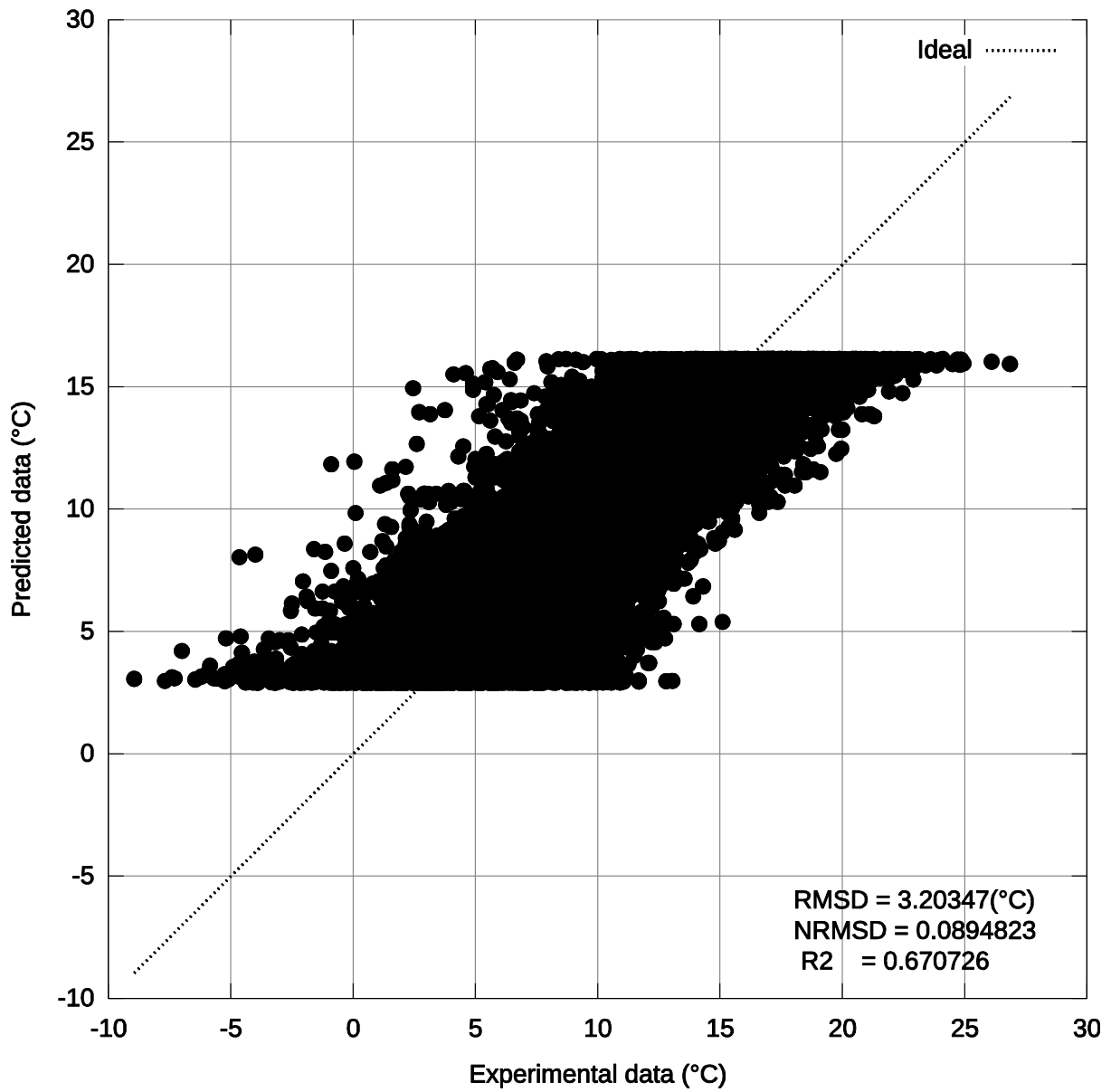
511 **Fig. 2** Comparison of stored energy calculated analytically using equation (7) and numerically

512 using equation (25) in a column of soil of 20 m for year 40th



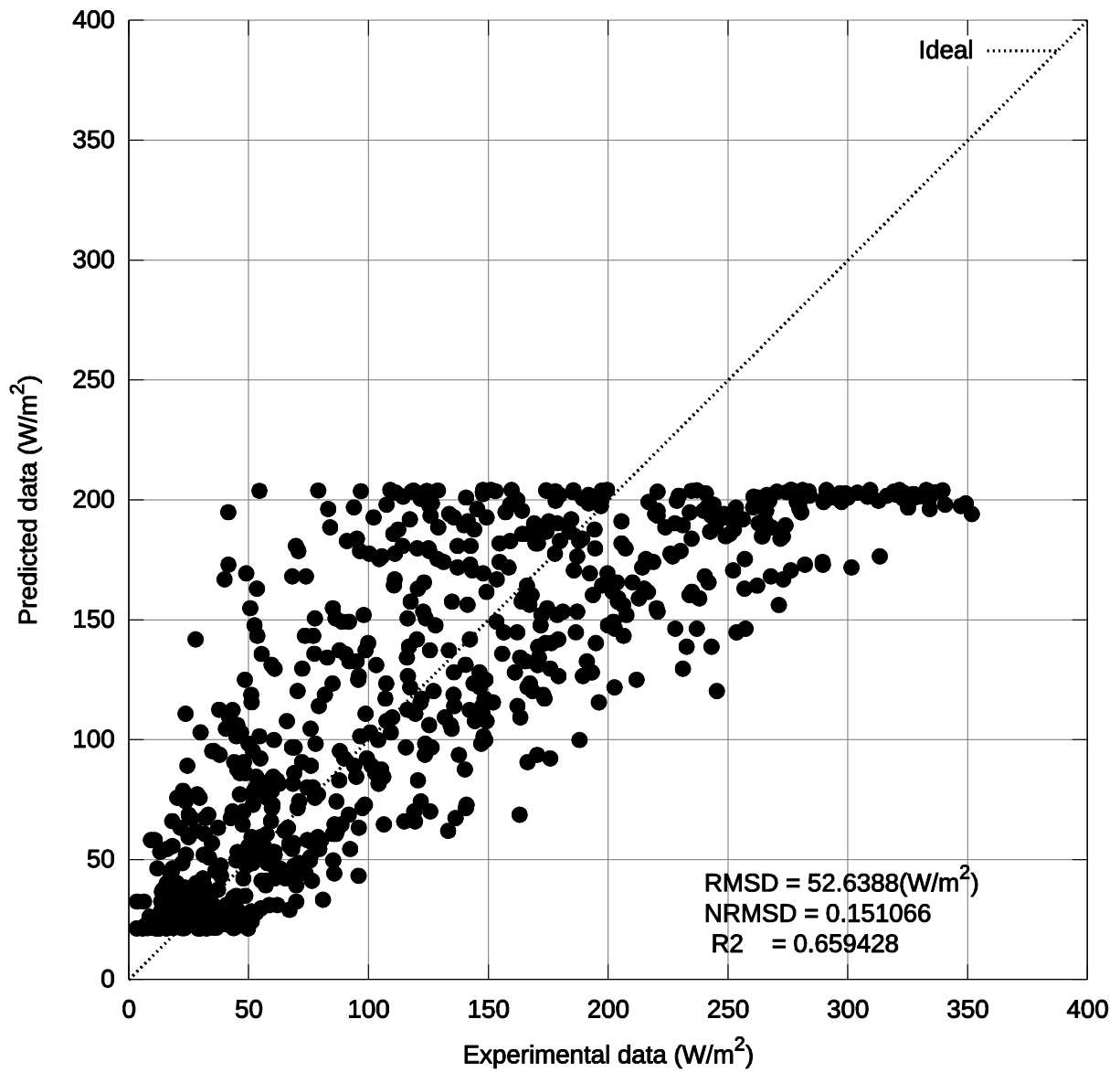
513

514 **Fig. 3** Comparison of daily average values for solar radiation predicted with equation (17) with
 515 data from (UK Meteorological Office 2012) for 1985-2004



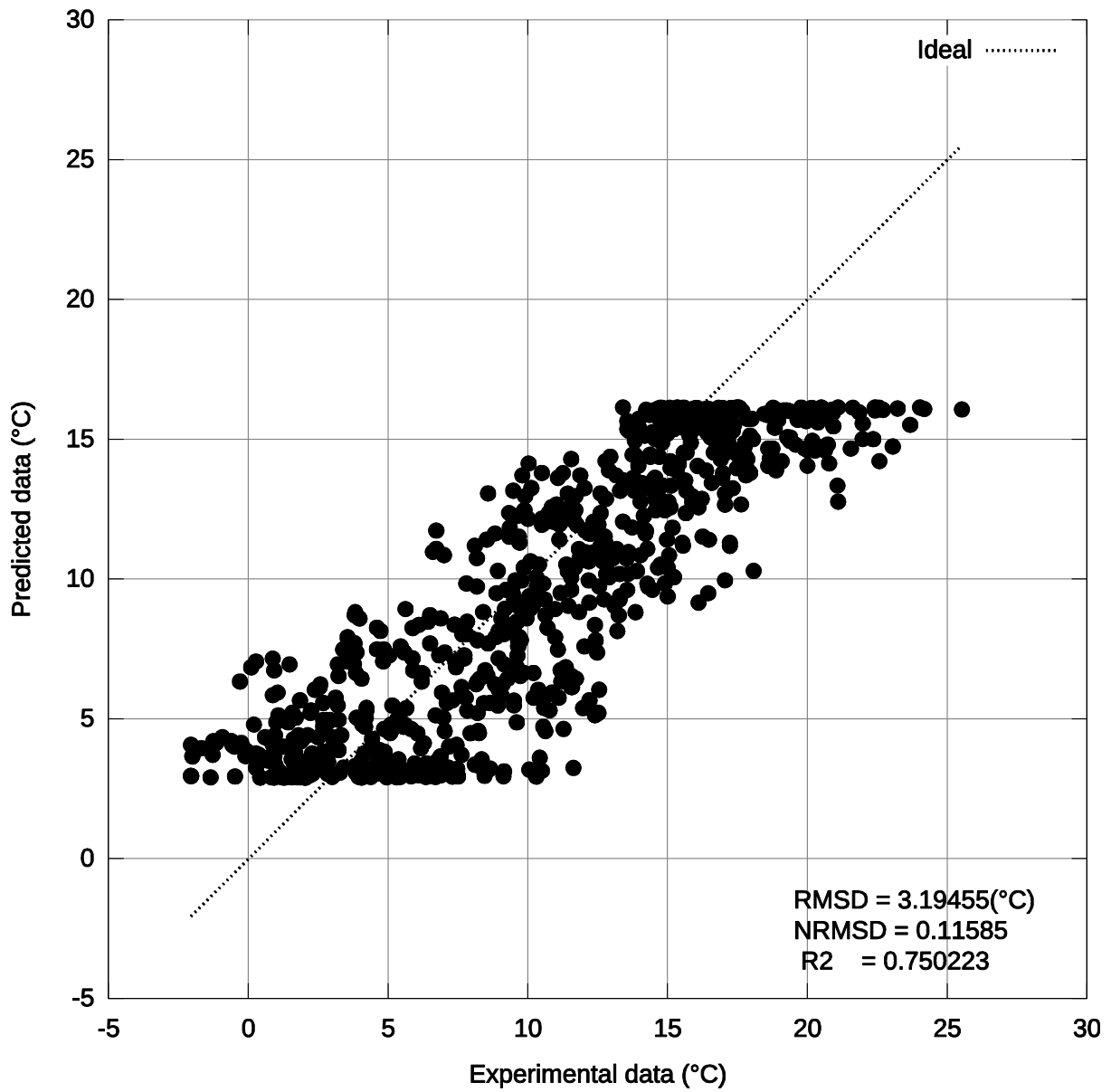
516

517 **Fig. 4** Comparison of daily average values for air temperature predicted with equation (20)
 518 with data from (UK Meteorological Office 2012) for 1985-2004



519

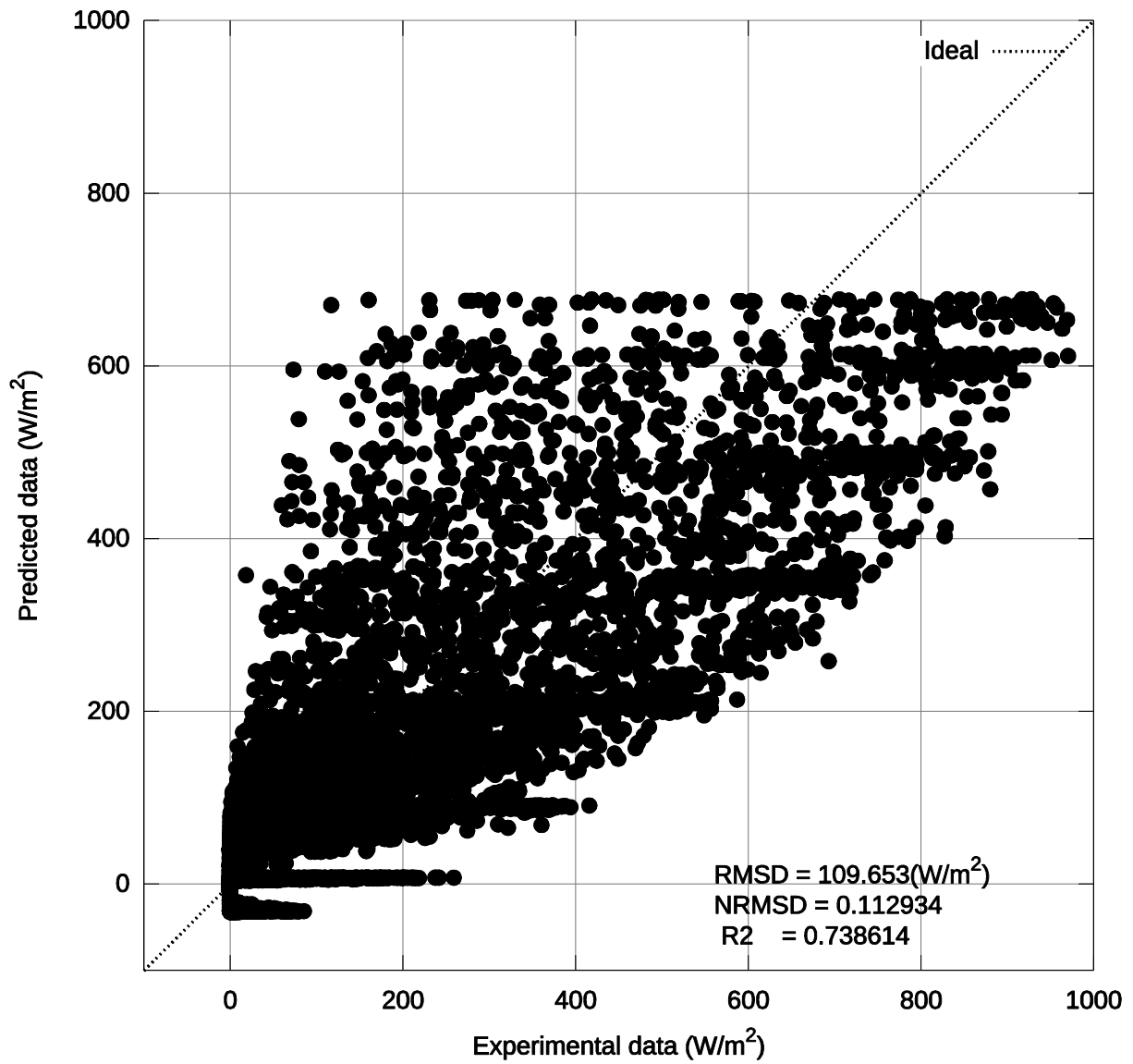
520 **Fig. 5** Comparison of daily average values for solar radiation predicted with equation (17) with
 521 data from (UK Meteorological Office 2012) for 2005-2006



522

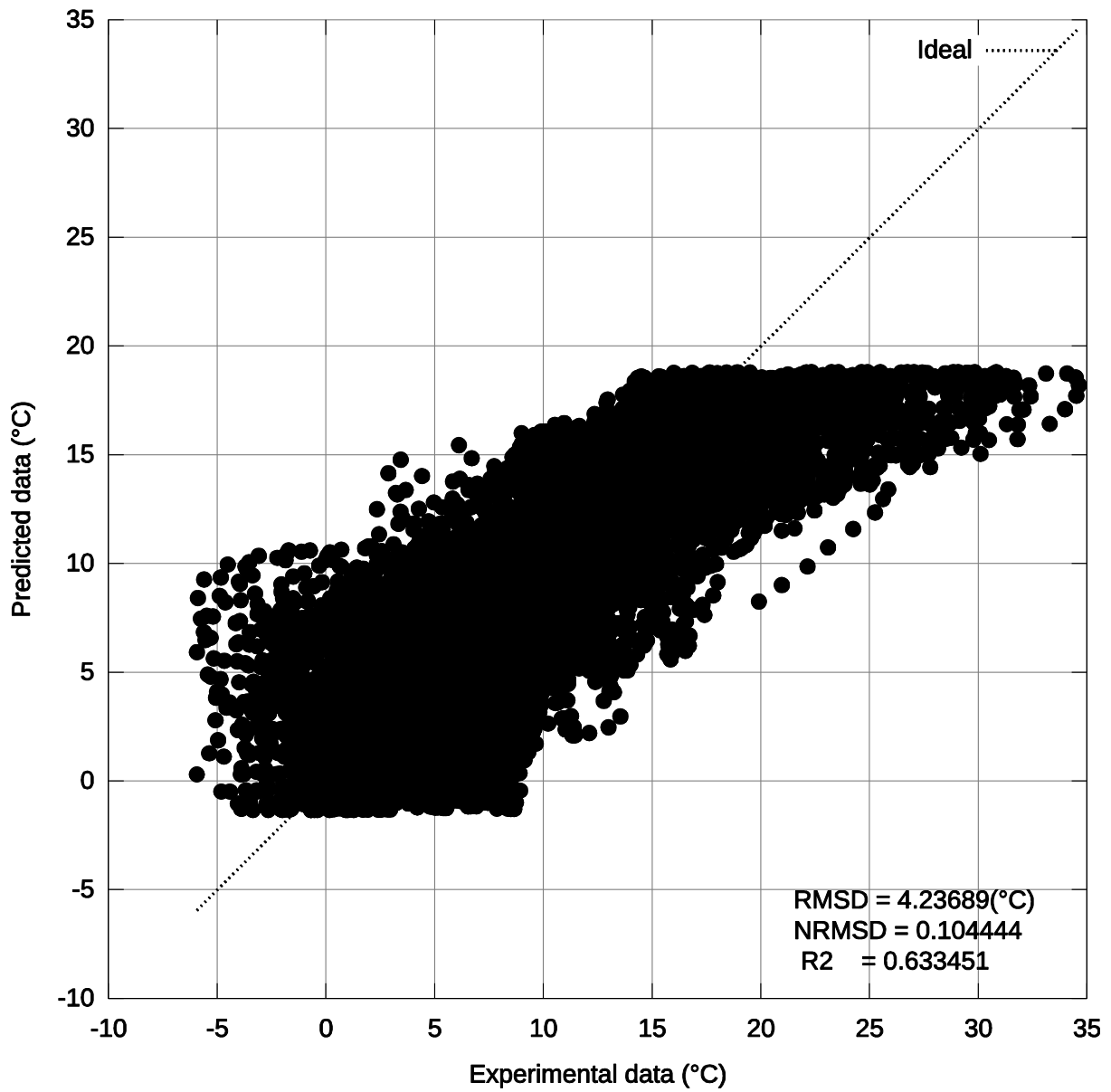
523 **Fig. 6** Comparison of daily average values for air temperature predicted with equation (20)

524 with data from (UK Meteorological Office 2012) for 2005-2006



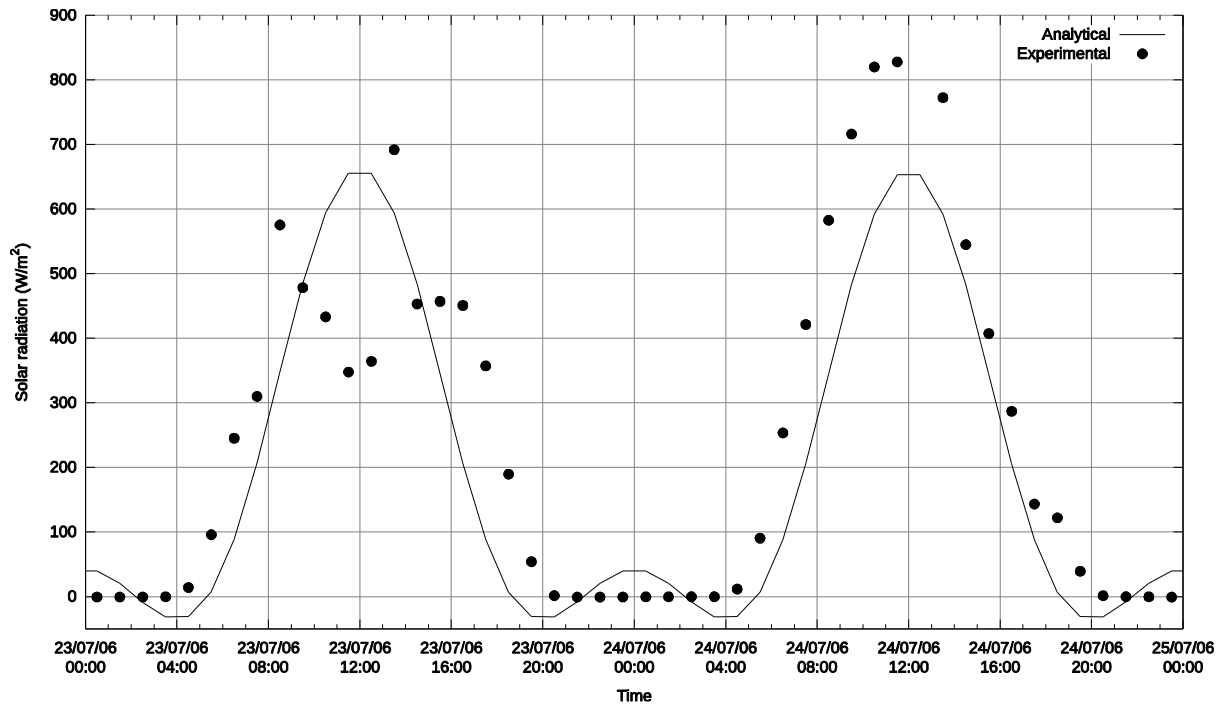
525

526 **Fig. 7** Comparison of hourly average values for solar radiation predicted with equation (17)
 527 with data measured on site provided by (Carder et al. 2007) from September 2005 to August
 528 2006



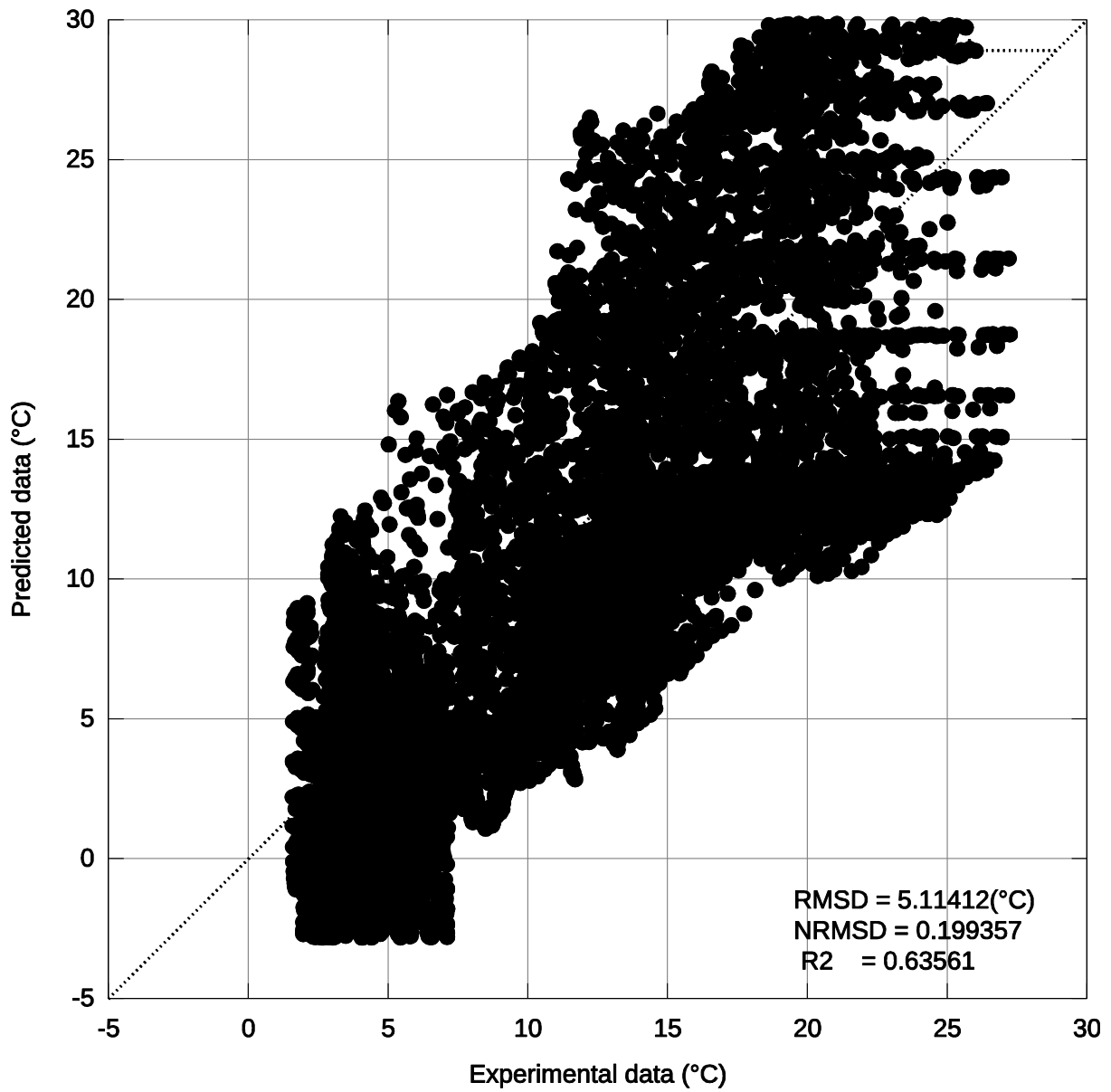
529

530 **Fig. 8** Comparison of hourly average values for air temperature predicted with equation (20)
 531 with data measured on site provided by (Carder et al. 2007) from September 2005 to August
 532 2006



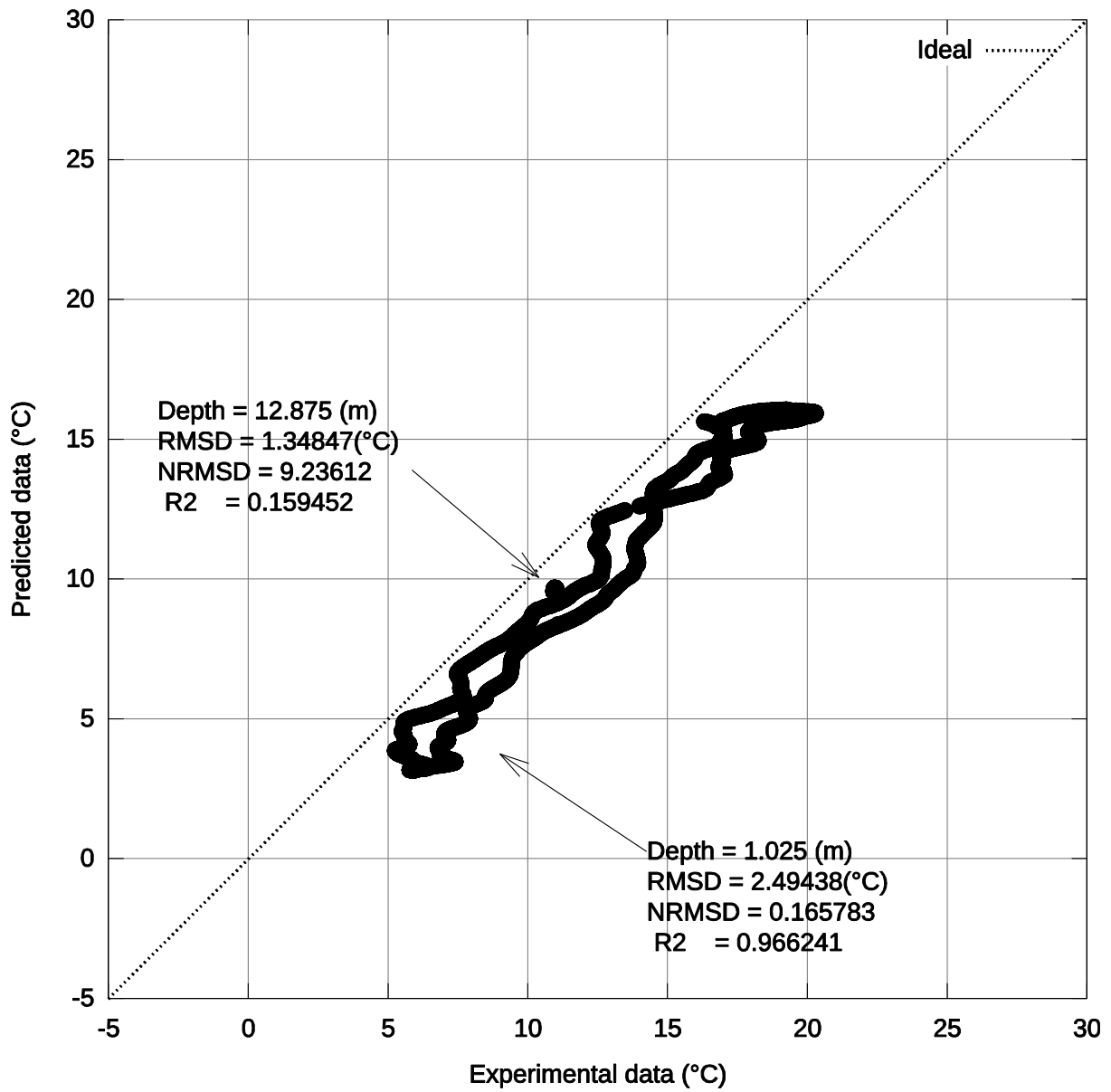
533

534 **Fig. 9** Comparison of solar radiation values predicted by equation (17) and measured on site
 535 by (Carder et al. 2007) for 2 days during summer 2006



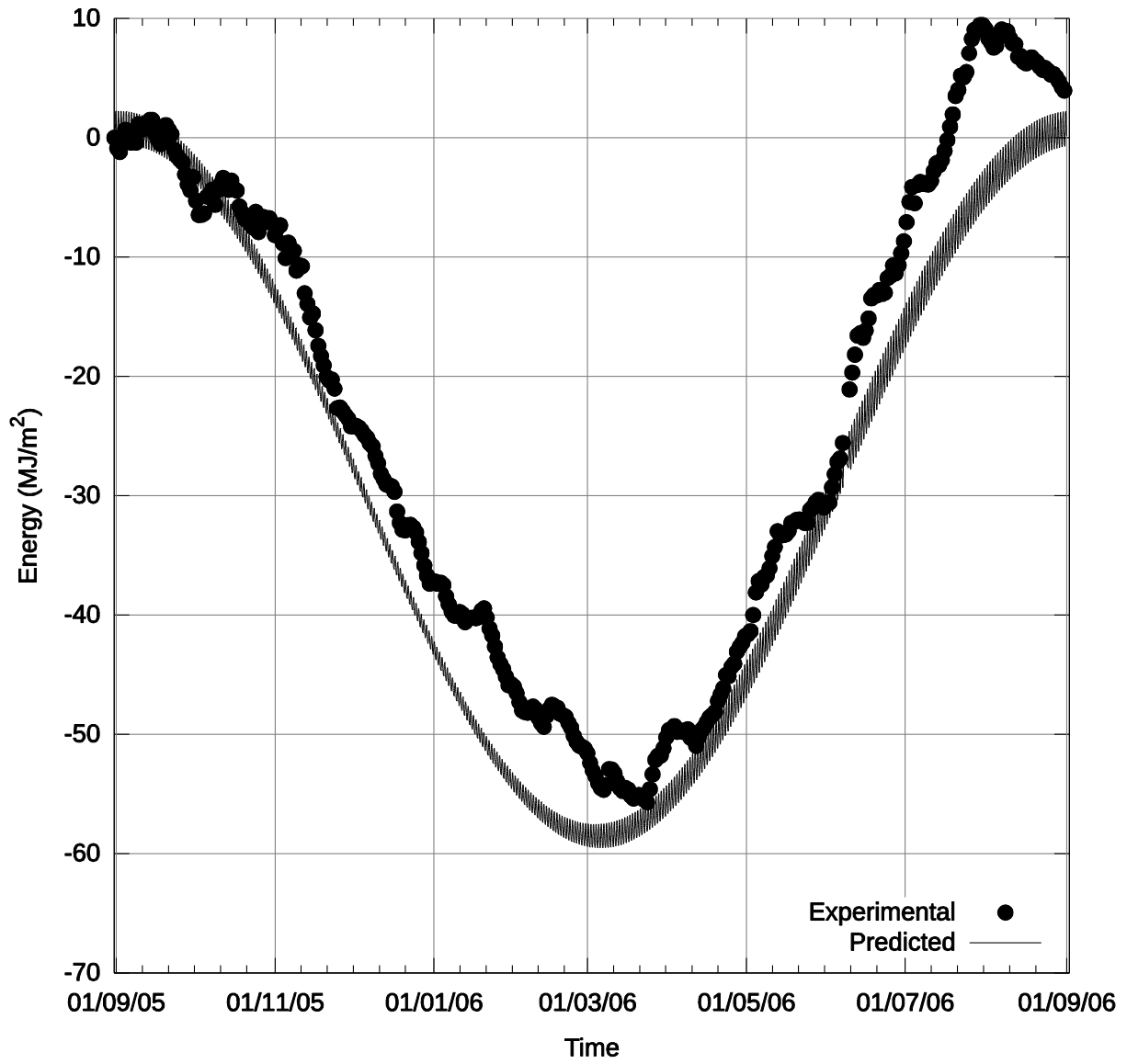
536

537 **Fig. 10** Comparison of predicted vs. experimental soil temperatures at 0.025 m depth for the
538 period September 2005 to August 2006



539

540 **Fig. 11** Comparison of predicted vs. experimental soil temperatures at 1.025 m and 12.875 m
 541 depth for the period September 2005 to August 2006



542

543 **Fig. 12** Transient variation of stored energy in a column of soil 12.875 m depth for the period

544 September 2005 to August 2006